COMMUNICATION

Photoactive Gate Dielectrics

By *Qian Shen, Linjun Wang, Song Liu, Yang Cao, Lin Gan, Xuefeng Guo,* Michael L. Steigerwald, Zhigang Shuai,* Zhongfan Liu,* and Colin Nuckolls**

Over the past decade, great progress has been made on organic thin-film transistors (OTFTs) with impressive achievements in improving carrier mobilities that are now comparable to those of amorphous silicon thin-film transistors.[1–4] However, it is still far from satisfactory requirements for real application. The focus of recent attention has been devoted to improving device performance and stability, reducing the power dissipation and fabrication cost, exploring new functionality, and developing simple fabrication techniques. Overcoming these challenges depends on the development of novel organic semiconductors and device optimization. From the point of the device, for the manufacture of high-quality OTFTs, the organic semiconductor is not the only critical component. It is also very important to incorporate the suitable gate dielectrics. In fact, OTFT performance can be substantially enhanced by manipulating the dielectric/semiconductor interfacial properties through gate dielectric optimization.[5–11] On the other hand, devices fabricated from hybrid gate dielectrics may offer the unique possibility of tailoring mechanical, electrical, and optical properties.[12–16] Therefore, rational design of gate dielectric functionalization, which aims to improve the device performance and/or install new functionalities into OTFTs, boosts development. Herein, we detail a smart method, by which organic transistor performance can be reversibly fine-tuned by lights with different wavelengths using photoactive gate dielectrics. Employing this interesting design, we have tested the efficient use of this concept for photoswitching the device performance of both *p*-type and *n*-type organic transistors on transparent, flexible, and foldable substrates.

This study builds on our recent work in which we showed that photochromic spiropyrans (SP) can be tethered to the surfaces of single-walled carbon nanotubes through molecular self-assembly[17] and combined with conductive polymers[18] to make

photosensitive devices. In both cases, UV- and visible-light irradiations can switch the device conductance back-and-forth between two distinct states by either reversible conformation-induced doping or proton transfer. Theoretical discussions[19] have suggested that the photoisomerization causes a significant change in the electric dipole moment (P_{mol}) of the molecule. Our density functional theory calculations show that in the closed form the electric dipole moment of the molecule is 6.4 D, while in the open form it is more than doubles to 13.9 D. Such a change in dipole moment could initiate a significant change in the electrostatic environment of the devices. We expected that photochromic SP when employed as one component of the gate dielectric, under illumination could alter the dielectric capacitance of the gate dielectric and therefore modulate the device performance.

A typical top-contact, bottom-gate OTFT device configuration was used in this study (**Figure 1**). Pentacene was selected as the model organic semiconductor because of its high mobility and the importance of this material for incorporation into electronic circuitry.[1–3] The photoactive gate dielectric was a hybrid polymer film [polymethyl methacrylate (PMMA) + SP, 150–1200 nm]. As control dielectrics, we used the corresponding thin films without the SP additive. We chose PMMA as the SP carrier. This provides buffering space for SP's conformational changes. It is an ideal polymer gate dielectric with good surface uniformity, low surface roughness, and relatively high capacitance for OTFTs.[5,20,21] On the other hand, the hydrophobic surface of hydroxyl-free PMMA could supply a surface energy close to that of pentacene.[8,21,22] All of these parameters favor growth of pentacene thin films that have the large grain size and this gives improved electrical characteristics of OTFTs. Tapping-mode atomic force microscopy (AFM) images obtained from the hybrid gate dielectric surfaces with different film thicknesses demonstrated smooth surface morphologies (maximum root mean square roughness ~0.3 nm) (Figure S1). After 40 nm pentacene deposition via thermal evaporation, this hybrid polymer dielectric allowed us to obtain very large pentacene crystal grains (~3 μm) with terraces (step heights about 15 Å) as demonstrated by AFM (Figure S1). In addition, X-ray diffraction measurements demonstrated the formation of highly crystal-quality pentacene thin films on top of the dielectric (Figure S2). These results are important to achieve the optimal OTFT performance.

UV–visible absorption studies show that SP molecules in thin films of the hybrid gate dielectric are able to reversibly switch back-and-forth between the neutral closed form (SP-closed) and the charge-separated, colored open form (SP-open) under UV- and visible-light irradiation (Figure S3). This indicates that PMMA can serve as a good matrix for SP molecules; it is rigid enough to be a structural support for the device, yet it

[*] Q. Shen, S. Liu, Y. Cao, L. Gan, Prof. X. Guo, Prof. Z. Liu
Beijing National Laboratory for Molecular Sciences
State Key Laboratory for Structural Chemistry
of Unstable and Stable Species
College of Chemistry and Molecular Engineering
Peking University, Beijing 100871 (P. R. China)
E-mail: guoxf@pku.edu.cn; zfliu@pku.edu.cn
L. Wang, Prof. Z. Shuai
Department of Chemistry
Tsinghua University
100084 Beijing (P. R. China)
E-mail: zgshuai@tsinghua.edu.cn
Dr. M. L. Steigerwald, Prof. C. Nuckolls
Department of Chemistry and the Columbia University
Energy Frontiers Research Center
Columbia University, New York, 10027 (USA)
E-mail: cn37@columbia.edu
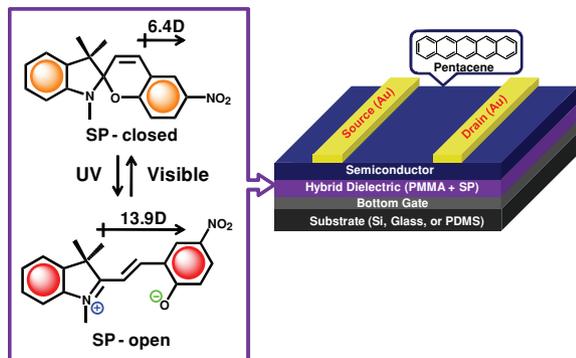
Figure 1. Schematic representation of the device structure showing how photochromic SP alter the dielectric capacitance for reversibly controlling the device performance under UV and visible light illumination.

is flexible enough to allow SP to isomerize. The calculated percent conversion of SP molecules from SP-close to SP-open at the photostationary state is ~57% (see the Supporting Information). Further AFM studies show that the transformation of SP molecules from SP-closed to SP-open under enough UV light irradiation did not change its surface uniformity and roughness at all, ensuring the successful fulfillment of the subsequent investigations (Figure S1C). Having understood the properties of the isolated dielectric, we then fabricated pentacene thin-film transistors on the hybrid gate–insulator substrates. Three types of substrates were used (Figure 1): silicon wafers for photoswitching studies, ITO glass for capacitance measurements, and polydimethyl-siloxane (PDMS) stamps for applications in flexible electronics.

To characterize the switching behavior of functionalized OTFTs, we used the hybrid dielectric with SP saturation concentration of ~7.0 × 10^{-2}M. We observed the formation of many SP microparticles in thin films of the hybrid dielectric when the SP concentration increased to ~7.5 × 10^{-2}M, and the molecular photochromism (and therefore the switching properties of the devices) is suppressed by the tight packing among neighboring molecules in SP microparticles.[18] To maximize the effect of SP on the device characteristics of the transistors, we used highly doped silicon wafers without silicon oxide layers as the sub-

strates (Figure 1). Dielectric films of various thicknesses were electrically characterized by using the sandwich electrode structures with gold pads (0.9 mm^2) on the surface of hybrid polymer films. The capacitances (C) and the saturation field-effect mobilities (μ) as a function of polymer thickness are summarized in **Figure 2**. Pentacene carrier mobility gradually decreased with the increase of polymer thickness, which is consistent with the results of the capacitance measurements. This is a sign of the field-dependent mobility. At similar voltages, there is less capacitive charge available to fill traps with thicker dielectrics. The average saturation carrier mobilities (μ_{max}) of these devices vary from ~1.9 × 10^{-2} to 1.7 × 10^{-3} cm^2 V^{-1}·s^{-1} when PMMA thickness increases. We notice that the average mobility of devices with a 150 nm thick hybrid polymer dielectric is lower than that of devices with a 300 nm thick PMMA thin film (~0.02 and 0.37 cm^2 V^{-1}·s^{-1}, respectively) although they have almost the similar capacitance. This might be due to the increase of the interface trap density in the presence of SP molecules.

We found that large and reversible changes in drain current occurred in these SP-functionalized OTFTs when SP isomerized between SP-closed and SP-open forms. **Figure 3A–E** shows such a representative photoswitching effect in a 40 nm pentacene thin film transistor with dielectric thickness of 1200 nm and SP concentration of ~7.0 × 10^{-2}M (Figure S5D). As shown in Figure 3A, after ~200 s of UV irradiation,[23] the initial (low) conductance state of the device (black curve, R_{on} = ~5.2 × 10^9 Ω at −50 V S/D bias and −30 V gate bias) was converted into a much higher conductance state (red curve, R_{on} = ~2.3 × 10^9 Ω). The reversion from SP-closed to SP-open was powered by visible light. After ~17 min of further visible-light irradiation (green curve in Figure 3A), the drain current of the device was essentially restored to its original value. We found that the back-and-forth phototswitching effect is rather gradual in time. Figure 3B and C shows the time evolution of the current–voltage curves during UV- and visible-light illumination, respectively. The similarity between the reversible photoswitching of the electrical conductivity of the functionalized devices and the reversible photoisomerization of SP molecules suggests that the photoswitching process of SP molecules is responsible for the changes in device characteristics of pentacene OTFTs. We noticed that SP photoisomerization was suppressed to different
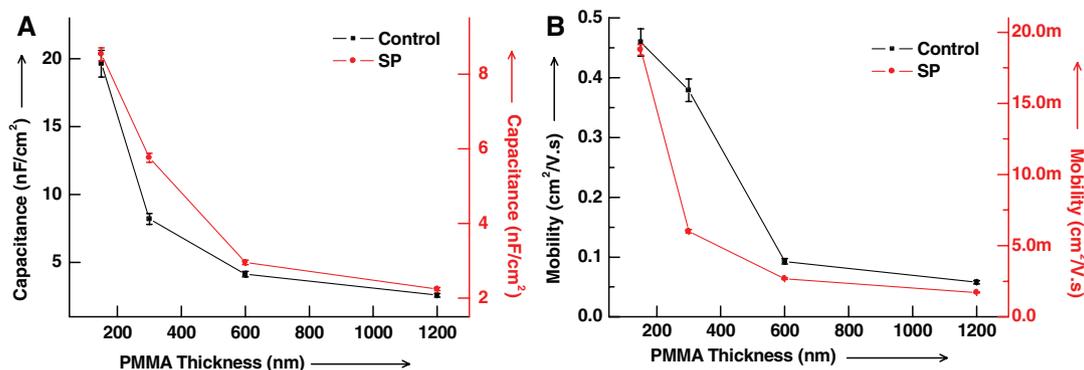
Figure 2. The capacitances (A) and the saturation field-effect mobilties (μ) (B) as a function of polymer thicknesses of devices built on silicon wafer substrates without SiO$_2$ thin films. The capacitance data were taken from Figure S4 at 1000 Hz frequency. Black curves are for control devices without SP molecules. Red curves are for devices with SP concentration of ~7.0 × 10^{-2}M.

WILEY InterScience®
DISCOVER SOMETHING GREAT
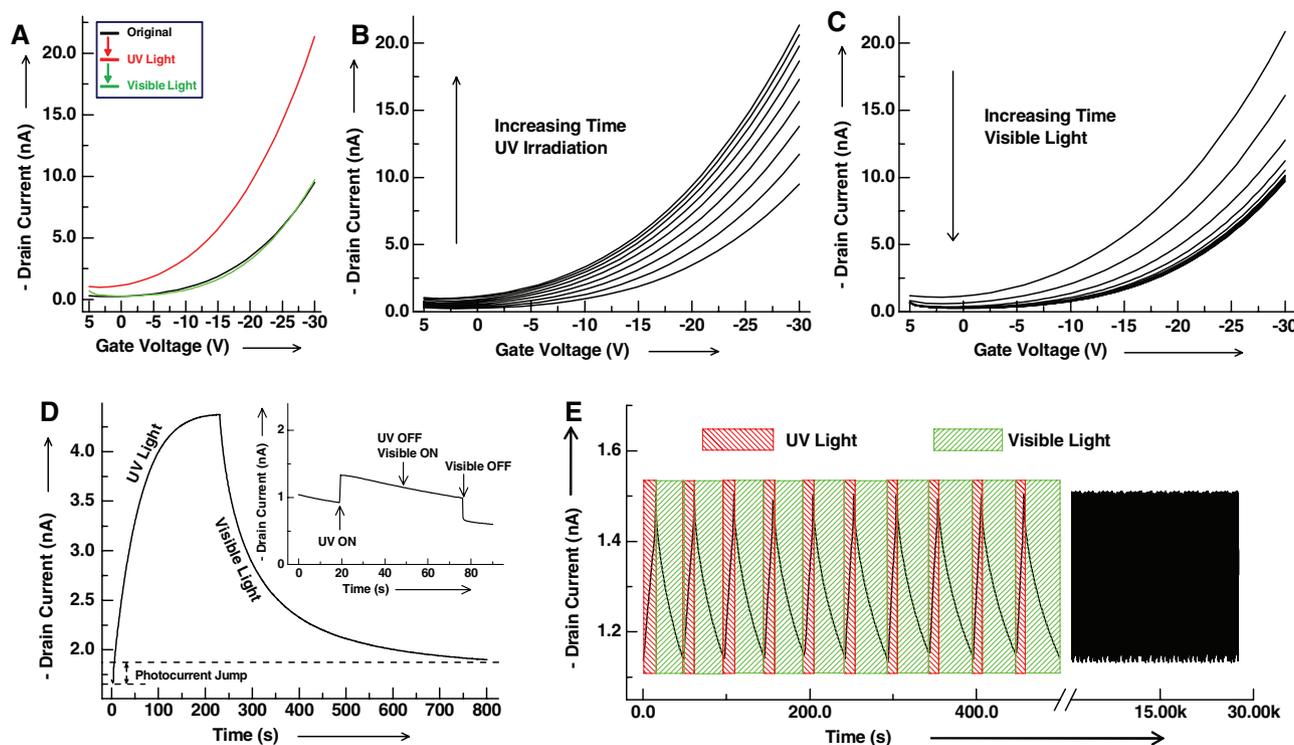
Figure 3. A) A representative photoswitching cycle in a 40 nm pentacene thin-film transistor with dielectric thickness of 1200 nm and SP concentration of ~7.0 × 10^{-2}M before UV irradiation (black), after UV irradiation (red), and after further visible irradiation (green). $V_{sd} = -50$ V. B,C) represent the gradual conversion between low- and high-conductance states when the current–voltage curves were taken every 25 s for UV illumination (B) and every 100 s for visible-light illumination (C). D) One full switching cycle of the time-dependent behavior of the same device. Inset: Time trace of the drain current for a control device (Figure S10) under irradiation of UV and visible lights ($V_{sd} = -20$ V and $V_g = -10$ V). E) Time trace of the drain current for the same device over a period of ~6 h with the first 10 cycles expanded for clarity, showing the reversible photoswitching events under irradiation of UV and visible lights ($V_{sd} = -50$ V, and $V_g = -30$ V).

extents when high gate bias voltages (above 60 V) were applied. This might be due to the damage of SP-open by the high electrical field during the photoswitching process. However, we found that all the devices worked well at less than 60 V gate bias voltage.

To gather kinetic data for the photoswitching process, we monitored the drain current as a function of time ($V_{sd} = -50$ V, $V_g = -30$ V) as the irradiation is toggled between UV and visible wavelengths. To clearly demonstrate the photoswitching process and mechanism discussed below, we do not show the slow back-conversion process of the devices in the dark after UV irradiation due to the slow transformation of SP from SP-open to SP-closed. Figure 3D shows one full switching cycle of the time-dependent behavior of the same device. A sudden current jump (~7% in the total current change) was also observed at the moment of turning on UV light generally due to the photoexcited state of organic semiconductors as proved by control experiments (Figure 3D, inset). In order to demonstrate the reversibility of the switching, we used shorter irradiation times. We found that these devices showed long-term operational stability in a perfectly reversible manner. Figure 3E demonstrates the switching cycles of the drain current as a function of time of the same device with the first 10 cycles expanded for clarity. After the measurements over a period of ~6 h and ~600 cycles, the devices still show the good switching effect and the original

transistor behaviors without obvious changes in mobility and on/off ratio (Figure S9). The kinetics of each process can be fit with a single exponential. Based on the data in Figure 3E, the overall rate contants in different parts were calculated, $K_{(UV)} = $~3.0 ± 0.2 × 10^{-2} s^{-1} and $K_{(visible)} = $~1.2 ± 0.2 × 10^{-2} s^{-1}. These kinetic results for the photoswitching process are very similar with or even faster than those we observed in our previous work.[17,18] More details for the other devices with the same device configuration but different PMMA thicknesses at SP concentration of ~7.0 × 10^{-2}M can be found in Figure S5–8.

To aid in the analysis of these results, we performed control experiments in which we measured the photoresponse of a pentacene device having the same polymer dielectric but lacking the spiropyran (Figure 3D, inset). During irradiation with either UV or visible light, we consistently observed the slow decrease in drain current, which was independent on PMMA thickness, probably resulting from problems associated with the device stability. From the trace in Figure 3D inset, the overall rate constants for each part were obtained, $K_{(UV)} \approx K_{(visible)} = $~5.0 ± 0.1 × 10^{-4} s^{-1}. In comparison with those in functionalized devices, two significant differences should be pointed out. One is that the rate constants of the device in Figure 3E under UV- and visible-light irradiation are two orders of magnitude larger than those obtained from the control device (Figure 3D, inset) under the same conditions. The other significant difference is that

the photoswitching effect under UV illumination in functionalized devices is opposite to that in the control devices. In addition, it is important to mention that the kinetic results for the conductance photoswitching process in functionalized devices discussed above are nearly the same as those of the SP photoisomerization obtained from UV–visible absorption studies (Figure S3). Therefore, it is quite clear that the photoisomerization of SP molecules is responsible for the switching effect in device characteristics.

After proving the interesting finding, we then turned our attention to studying the switching mechanism. We first tested the photoswitching effect of the functionalized devices fabricated on transparent ITO glass substrates. These devices have the same device configuration as shown in Figure 1 with a hybrid polymer dielectric at SP concentration of ~7.0 × 10^{-2}M and PMMA thickness of 1200 nm, which was comprehensively studied above. The maximum carrier mobility (μ_{max}) obtained from these devices is ~3.3 × 10^{-3} cm^2 V·s^{-1}. We observed the same photoswitching effect of SP molecules on device characteristics in these devices. Details can be found in the Supporting Information (Figure S12).

We have performed molecular dynamics (MD) simulations within the Materials Studio software platform to evaluate the static dielectric constants by the dipole moment fluctuation properties. The details of system construction and MD simulation can be found in the Supporting Information. With this approach, the converged dielectric constant of the system with SP-closed was calculated to be 2.87 (**Figure 4**), which is in good agreement with the experimental data of ~2.84. Importantly, we found that the calculated dielectric constant in the SP-open case is 3.67, which is ~28% larger than that in the SP-closed case. Consequently, based on the above theory and the observed experimental results, we hypothesize that the SP photoisomerization could initiate the reversible changes in capacitance of the hybrid gate dielectric and thus modulate the electrical conductivity of the devices since it can induce a large change in dipole moment of SP molecules and SP molecules serve as the key component of the gate dielectric.

To prove this hypothesis, we characterized the electrical properties of the hybrid dielectric using sandwich device

Figure 4. Simulated static dielectric constant as a function of time for the systems with SP-closed (black) and SP-open (red) molecules using five configurations.

architectures (gold pad (0.9 mm^2) top electrode and ITO film bottom electrode). In this case, we irradiated the material through the bottom of ITO transparent electrodes. **Figure 5A,B** shows the time-dependent evolution of the capacitance curves of a hybrid polymer dielectric at SP concentration of ~7.0 × 10^{-2}M and PMMA thickness of 1200 nm. It is remarkable that there is a gradual transition from low to high capacitance states when the device is exposed to UV light. The capacitance increased sharply at the beginning of UV irradiation and then saturated after ~220 s of exposure. Similarly, the recovery process is powered by visible light irradiation. In Figure 5B, we show that the capacitance sharply decreased initially and then slowly attenuated, completing a full switching cycle after ~15 min of further exposure to visible light. Very importantly, the photoswitching processes of the devices are reversible. In Figure 5C, we show four representative full switching cycles of the same device by taking the data at 1 MHz frequency. In principle, the switching reversibility can be optimized by using shorter irradiation times or milder measurement conditions. Based on the data in Figure 5C, we can calculate the corresponding field effect mobility of the device used in Figure S12A. As shown in Figure 5D, the device nicely switched its mobility back-and-forth between two distinct states. The photoswitching in both capacitance and mobility is perfectly consistent with that in conductivity discussed above. In control experiments where we used only PMMA thin films with the same thickness as the dielectric, we observed only the negligible increases in capacitance under either UV- or visible-light irradiation (Figure S13), which might be due to the slight effect of the dissociative photoexcitation of C–C or C–H bonds of polymer PMMA on capacitance.[24,25] By comparing the photoswitching results obtained from the hybrid polymer dielectric with those from the control polymer dielectric, we are confident that the photoisomerization of the SP molecules are responsible for the photoswitching of the capacitance in devices. Since SP photoisomerization can induce a big change in dipole moment of individual molecules and SP molecules serve as the key component of the gate dielectric, it is reasonable that this dipole change could initiate a collective change in dielectric constant of the gate dielectric, thus leading to the reversible photomodulation of the capacitance of the gate dielectric. It was reported that modification of the capacitance of the gate dielectric is an efficient approach to substantially improving the drain current.[7] The gate dielectric with the higher capacitance value can store more charges at the semiconductor/dielectric interface at similar voltages, which leads to the increases of the carrier density and then the drain current in the devices. As is evident in the equation for the mobility calculation (see the Supporting Information), these effects may result in the considerable improvement of the device mobility. Consequently, it is not surprising that SP photoisomerization can realize the reversible photoregulation of the device characteristics (conductivity and mobility) of the devices as demonstrated experimentally through a novel conformation-induced capacitive coupling mechanism. Another important feature that should be mentioned is that all of the conformational changes happen within the gate dielectric layer driven by the most convenient and noninvasive tool of lights without any damage of the semiconductors, making the functioning devices extremely stable as shown in Figure 3E. However, the percent
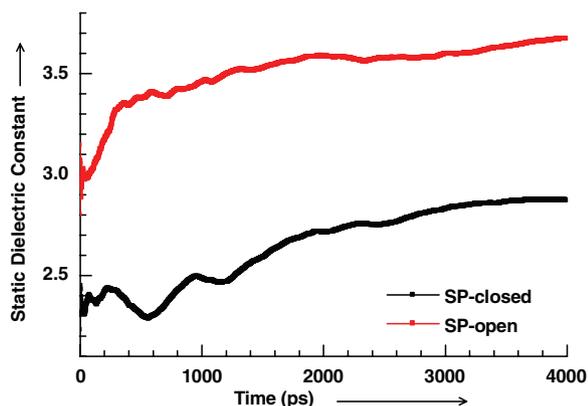
Adv. Mater. 2010, 22, 3282–3287
© 2010 WILEY-VCH Verlag GmbH & Co. KGaA, Weinheim

WILEY
InterScience®
DISCOVER SOMETHING GREAT

3285
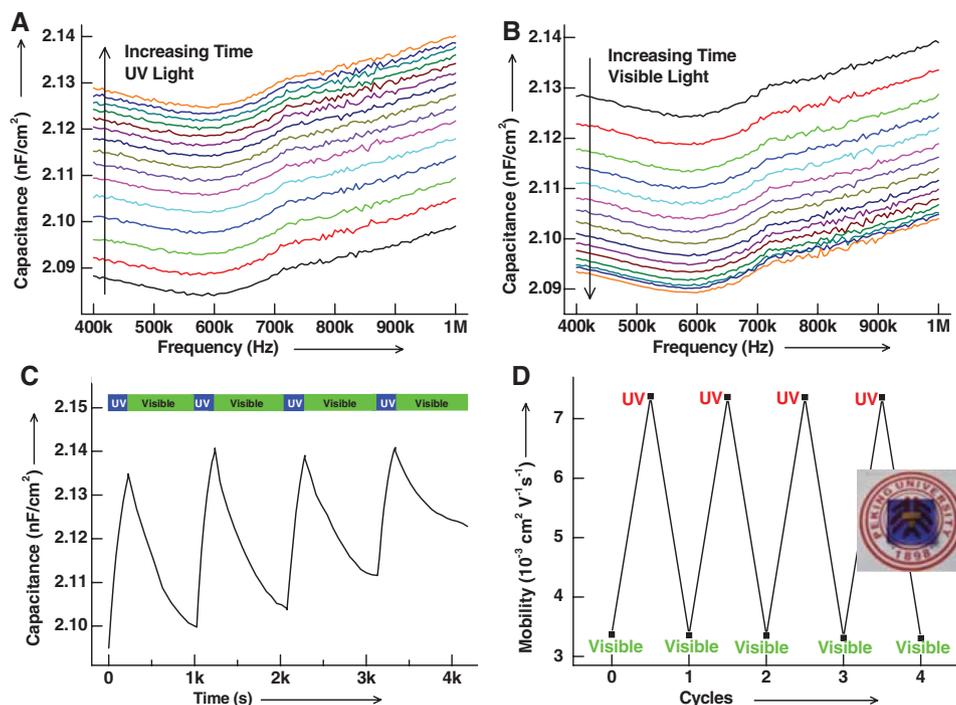
Figure 5. Demonstration of switching mechanisms. A,B) The gradual transition of the capacitances of a hybrid polymer dielectric between low- and high-capacitance states when the curves were taken every 15 s for UV irradiation (A) and every 60 s for visible irradiation (B). The SP concentration is ~7.0 × 10⁻²M and the PMMA thickness is 1200 nm. C) The representative four full switching cycles of the same device by taking the data at 1 MHz frequency. D) The corresponding representative switching cycles of the mobility of a device used in figure S12A. Inset: an optical image of this device fabricated on an ITO glass substrate.

change (~2%) in capacitance obtained from real experiments is less than that predicted by the theory (~28%) probably due to the unoptimized operation conditions and the incomplete conversion of SP molecules from SP-close to SP-open (~57%). Further study is needed to understand the precise photoswitching mechanisms, which are of crucial importance to improve the device performance.

To explore the feasible application of this concept in flexible electronics, we used PDMS stamps as flexible and foldable substrates. In this experiment, we first deposited a 100 nm Au thin film on PDMS substrates as the gate electrode and then fabricated standard pentacene transistors with a hybrid polymer dielectric at SP concentration of ~7.0 × 10⁻²M and PMMA thickness of 1200 nm. As shown in Figure S14B, all the devices displayed the similar reversible photoswitching effect under the same measurement conditions. Finally, to test the generality of this mechanism, we used an n-type semiconductor, F₁₆CuPc, to make 40 nm thin-film transistors on ITO glass substrates with the same gate dielectric. For this example, a time trace of the drain current in such a device clearly showed photoswitching under UV- and visible-light irradiation (Figure S15B).

The present results elaborate an unprecedented and general phenomenon of molecular conformational transformation effect of crucial consequences on the charge transport properties of underlying OTFTs when a photochromic molecule SP integrated with polymer PMMA is used as photoactive gate dielectrics, and demonstrate a novel mechanism of conformation-induced capacitive coupling of great importance for fine-tuning

the device performance of OTFTs. As predicted theoretically, reversible and significant capacitance and thus mobility transitions are universally observed experimentally in devices built on either rigid or flexible substrates using either p-type or n-type semiconductors when the SP molecules are toggled back-and-forth between two distinct conformational states under UV- or visible-light irradiation. Since SP photoisomerizations happen only within the gate dielectric layer and the most convenient and noninvasive tool of lights is used, organic semiconductors are essentially untouched without any damage, thus significantly improving the device stability in comparison with the cases based on the sorption-based sensing mechanism.[26] This forms the basis for new types of ultrasensitive devices for chemical and environmental sensing in a noninvasive manner. On the other hand, integrating molecular functionalities into OTFTs suggests a new and sensitive methodology for amplifying molecular conformation information into the detectable electrical signals and exploring fundamental properties of molecular conformation dynamics. We expect that these results should offer new opportunities of designing more rational fabrication of multifunctional molecular sensors and devices.

Supporting Information

Supporting Information is available online from Wiley InterScience or from the author.

Acknowledgements

[1] A. R. Murphy, J. M. J. Frechet, *Chem. Rev.* **2007**, *107*, 1066.

[2] C. R. Kagan, P. Andry, *Thin-film Transistors*, Dekker, New York **2003**.

[3] J. Zaumseil, H. Sirringhaus, *Chem. Rev.* **2007**, *107*, 1296.

[4] C. Reese, Z. Bao, *Mater. Today* **2007**, *10*, 20.

[5] C. Kim, A. Facchetti, T. J. Marks, *Science* **2007**, *318*, 76.

[6] A. Facchetti, M.-H. Yoon, T. J. Marks, *Adv. Mater* **2005**, *17*, 1705.

[7] S. A. DiBenedetto, A. Facchetti, M. A. Ratner, T. J. Marks, *Adv. Mater.* **2009**, *21*, 1407.

[8] L.-L. Chua, J. Zaumseil, J.-F. Chang, E. C. W. Ou, P. K. H. Ho, H. Sirringhaus, R. H. Friend, *Nature* **2005**, *434*, 194.

[9] H. Klauk, U. Zschieschang, J. Pflaum, M. Halik, *Nature* **2007**, *445*, 745.

[10] M. J. Panzer, C. D. Frisbie, *Adv. Mater.* **2008**, *20*, 3177.

[11] A. Salleo, M. L. Chabinyc, M. S. Yang, R. A. Street, *Appl. Phys. Lett.* **2002**, *81*, 4383.

[12] Y. Guo, C. Di, S. Ye, X. Sun, J. Zheng, Y. Wen, W. Wu, G. Yu, Y. Liu, *Adv. Mater.* **2009**, *21*, 1954.

[13] K.-J. Baeg, Y.-Y. Noh, J. Ghim, S.-J. Kang, H. Lee, D.-Y. Kim, *Adv. Mater.* **2006**, *18*, 3179.

[14] T. B. Singh, N. Marjanovic, G. J. Matt, N. S. Sariciftci, R. Schwodiauer, S. Bauer, *Appl. Phys. Lett.* **2004**, *85*, 5409.

[15] R. Schroeder, L. A. Majewski, M. Grell, *Adv. Mater.* **2004**, *16*, 633.

[16] P. Liu, Y. Wu, Y. Li, B. S. Ong, S. Zhu, *J. Am. Chem. Soc.* **2006**, *128*, 4554.

[17] X. Guo, L. Huang, S. O'Brien, P. Kim, C. Nuckolls, *J. Am. Chem. Soc.* **2005**, *127*, 15045.

[18] X. Guo, D. Zhang, G. Yu, M. Wan, J. Li, Y. Liu, D. Zhu, *Adv. Mater.* **2004**, *16*, 636.

[19] M. Sun, F. Ma, *J. Theor. Comput. Chem.* **2006**, *5*, 163.

[20] J. C. Pinto, G. L. Whiting, S. Khodabakhsh, L. Torre, A. B. Rodriguez, R. M. Dalgliesh, A. M. Higgins, J. W. Andreasen, M. M. Nielsen, M. Geoghegan, W. T. S. Huck, H. Sirringhaus, *Adv. Funct. Mater.* **2008**, *18*, 36.

[21] A. L. Deman, M. Erouel, D. Lallemand, M. Phaner-Goutorbe, P. Lang, J. Tardy, *J. Non-Cryst. Solids* **2008**, *354*, 1598.

[22] F. Todescato, R. Capelli, F. Dinelli, M. Murgia, N. Camaioni, M. Yang, R. Bozio, M. Muccini, *J. Phys. Chem. B* **2008**, *112*, 10130.

[23] Details of materials and measurement methods can be found in the Supporting Information.

[24] N. Benson, M. Schidleja, C. Melzer, R. Schmechel, H. von Seggern, *Appl. Phys. Lett.* **2006**, *89*, 182105.

[25] A. Hollander, J. E. Klemberg-Sapieha, M. R. Wertheimer, *Macromolecules* **1994**, *27*, 2893.

[26] M. E. Roberts, S. C. B. Mannsfeld, N. Queralto, C. Reese, J. Locklin, W. Knoll, Z. Bao, *Proc. Natl. Acad. Sci. USA* **2008**, *105*, 12134.